

Spoof Surface Plasmon Polariton Modes Propagating Along Periodically Corrugated Wires

A. I. Fernández-Domínguez, L. Martín-Moreno, F. J. García-Vidal, S. R. Andrews, and S. A. Maier

(Invited Paper)

Abstract—In this paper, we analyze in detail the characteristics of surface electromagnetic modes that can propagate along a periodically corrugated, perfectly conducting wire. We show how these modes, termed *spoof surface plasmon polaritons*, resemble surface plasmon polaritons supported by metallic wires at optical frequencies. The important point is that the dispersion relation of spoof surface plasmon polaritons is mainly controlled by the geometry of the corrugation. This fact allows the tuning of the properties of these modes via changes in corrugation geometry. Important applications lie in high-confinement waveguiding at far-infrared and microwave frequencies, including the possibility of efficient propagation to the tip of tapered structures for focusing.

Index Terms—Focusing, plasmonics, terahertz radiation.

I. INTRODUCTION

THE ABILITY to localize electromagnetic energy to below the diffraction limit of classical optics via the exploitation of surface plasmon–polaritons (SPPs)—electromagnetic surface waves sustained at the interface between a conductor and a dielectric [1]—is currently being exploited in a plethora of studies spanning from photonics, optoelectronics, and materials science to biological imaging and biomedicine [2]. While the basic physics of SPPs has been described in a number of seminal papers spanning the last century [3]–[5], the more recent emergence of powerful nanofabrication and characterization tools has catalyzed a vast interest in their study and exploitation. The dedicated field of plasmonics [6] is now firmly established not only within the photonics community, but bringing together researchers and technologists from a variety of disciplines wanting to take advantage of subwavelength light localization effects in the near field of the conductor.

Most interest is understandably focused on the spectral regime, where SPPs are strongly confined to the respective conductor/dielectric interface, i.e., where subwavelength mode

localization is achieved in the direction perpendicular to the interface. The same holds true for more complex geometries, such as metallic slabs, wires, or particle arrays, where the high field localization and concomitant field enhancement has been utilized, for example, for optical nanowaveguides [7]–[12] or single-molecule Raman spectroscopy [13], [14]. These strongly confined SPPs occur at frequencies, which are still an appreciable fraction of the intrinsic plasma frequency of the conductor in question. In a simple picture, here the motion of the conduction electrons at the interface shows an appreciable phase lag with respect to the driving electromagnetic fields, leading to a reduction in both phase and group velocity of the SPP, and therefore, to strong localization. An appreciable fraction of the SPP field energy resides inside the conductor, causing the well-known tradeoff between localization and loss.

Most plasmonics research has thus far focused on the noble metals Ag, Au, and Cu, which show plasma frequencies in the UV. Therefore, the aforementioned strong localization is only achieved for visible frequencies. As the frequency gets lowered from the near-infrared to the microwave regime of the electromagnetic spectrum, the field localization to the interface decreases (on the dielectric side) from the subwavelength regime to distances of many wavelengths, and SPPs acquire the character of a grazing-incidence light field, with phase velocities asymptoting the phase velocity of light in the dielectric. It is interesting that the first theoretical descriptions of SPPs treated this regime, namely the seminal publications by Sommerfeld [3] and Zenneck [15] on electromagnetic surface wave propagation at radio frequencies along cylindrical metal wires and planar metal interfaces. The link with more localized SPP excited via optical beams on diffraction gratings [4] or via electron impact [5] occurred only decades later.

Recently, there has been a resurgence of interest into SPP propagation along metal wires in the terahertz (THz) regime of the spectrum [16], [17], mostly in a context of biochemical sensing. However, the delocalized nature of the Sommerfeld waves (typical wavelength $\lambda = 300 \mu\text{m}$ at 1 THz, yet the fields extend over many millimetres away from the wire) sets constraints upon the achievable sensitivity, and leads to significant radiation loss at bends and surface imperfections. Generally, the field confinement decreases with increasing conductivity of the conductor, and in the limit of a perfect electrical conductor, planar interfaces and wires do not sustain electromagnetic surface waves anymore (in the later case, for azimuthally independent modes).

It would be highly desirable—also in a context of waveguiding—if stronger localization to wavelength and

Manuscript received December 6, 2007. First published April 3, 2008; current version published December 24, 2008. This work was supported in part by the Air Force Office of Scientific Research under Grant FA9550-07-1-0441 and Grant FA8655-07-1-3045, in part by the Royal Society, and in part by the Spanish MEC under Grant MAT2005-06608-C02.

A. I. Fernández-Domínguez and F. J. García-Vidal are with the Department of Theoretical Condensed Matter Physics, Universidad; Autonoma de Madrid, 28049 Madrid, Spain (e-mail: anisaac.fernandez@uam.es; fj.garcia@uam.es).

L. Martín-Moreno is with the Department of Condensed Matter Physics, Universidad de Zaragoza, 50009 Zaragoza, Spain (e-mail: lmm@unizar.es).

S. R. Andrews is with the Department of Physics, University of Bath, Bath BA2 7AY, U.K. (e-mail: s.r.andrews@bath.ac.uk).

S. A. Maier is with the Department of Physics, Imperial College, London SW7 2AZ, U.K. (e-mail: s.maier@imperial.ac.uk).

Color versions of one or more of the figures in this paper are available online at <http://ieeexplore.ieee.org>.

Digital Object Identifier 10.1109/JSTQE.2008.918107

subwavelength dimensions could also be achieved in this spectral regime with metallic guiding modalities. This is indeed possible if the metallic interfaces show subwavelength structure, even in the limit of perfect conductivity [18]–[20]. This can be understood by realizing that the subwavelength surface structure is not directly sampled by the wave, and can therefore, be seen as an effective medium surface layer, applying effectively the concept of metamaterials. THz surface waves with stronger localization than expected for Sommerfeld waves have, for example, been observed on thin metallic meshes [21]. For planar interfaces structured with 2-D arrays of holes or 1-D arrays of grooves, it can be shown that this effective surface layer can be described with a dielectric permittivity of the Drude form, with the plasma frequency entirely controlled by geometry [22]–[24]. This way, a plasma frequency in the THz regime of the spectrum can be achieved for metallic interfaces structured in easily realizable geometries [25]. In the perfect conductor limit, these designed surface waves are known as *spoof* surface plasmon polaritons.

Our paper is structured as follows. In Section II, we briefly analyze in a didactical nature the mode characteristics of surface plasmon polaritons propagating along wires of finite conductivity. The concept of spoof plasmons applied to wires is then introduced in Section III, which presents a detailed analytical model of their dispersion and mode profile. Examples for guiding and focusing are briefly discussed in Section IV, followed by concluding remarks.

II. AZYMUTHALLY-INDEPENDENT SURFACE PLASMON POLARITONS ON METALLIC WIRES

In this section, we analyze the properties of azimuthally-independent SPPs propagating along the surface of metallic cylindrical wires (the so-called Sommerfeld waves [3], [26], [27]). The rotational symmetry implies that the electromagnetic (EM) fields do not depend on θ (where θ is the azimuthal angle), leading to a decoupling of both light polarizations (*s* and *p*). Since SPPs are transverse magnetic (TM) modes, we restrict our study to *p*-polarized light, i.e., magnetic field normal to the wire axis (*z*-direction). In each region of the structure, we write the relevant field components (E_z and H_θ) in terms of the corresponding solutions of Maxwell equations. Thus, in the vacuum region surrounding the wire, we have

$$\begin{aligned} E_z^V(r, z) &= E_V K_0(q_V r) e^{ik_z z} \\ H_\theta^V(r, z) &= Y_V(k_z) E_V K_1(q_V r) e^{ik_z z} \end{aligned} \quad (1)$$

where $k_0 = \omega/c$ is the wave vector modulus and $q_V = \sqrt{k_z^2 - k_0^2}$ its radial component. The decaying behavior of the EM fields with increasing r is given by the modified Bessel functions of the second kind K_0 and K_1 , whereas the mode admittance is $Y_V(k_z) = ik_0/q_V$.

Inside the metallic wire, EM fields must decay inward with increasing distance from the wire surface (decreasing r). They can be expressed as

$$\begin{aligned} E_z^M(r, z) &= E_M I_0(q_M r) e^{ik_z z} \\ H_\theta^M(r, z) &= Y_M(k_z) E_M I_1(q_M r) e^{ik_z z} \end{aligned} \quad (2)$$

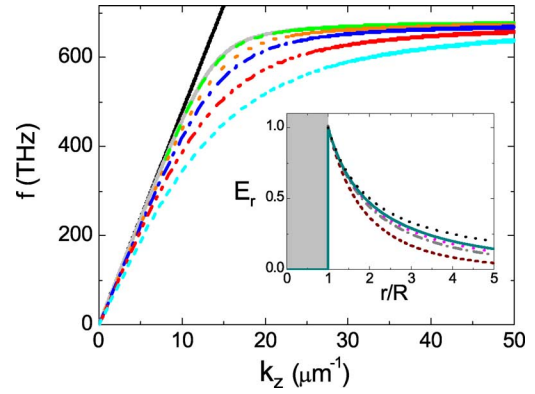


Fig. 1. Dispersion Relation of SPPs on lossless Au wires of different radii (R): 10 μm (dashed line), 3 μm (dotted line), 0.2 μm (dotted-dashed line), 0.1 μm (dashed-doubled-dotted line), and 0.05 μm (short dashed line). Inset: Radial component of the electric field versus r for the SPPs supported by metallic wires ($R = 0.35 \mu\text{m}$, $f = 330$ THz) with different dielectric constants: $\epsilon = -34$ (short dashed line), $\epsilon = -200$ (dotted-dashed line), $\epsilon = -400$ (dotted line), and $\epsilon = -1000$ (solid line).

where now $q_M = \sqrt{k_z^2 - \epsilon(\omega)k_0^2}$ is the wave vector radial component into the wire, and $\epsilon(\omega)$ is the metal dielectric function. The radial dependence of the EM fields is now given by the modified Bessel functions of the first kind, I_0 and I_1 . Finally, the mode admittance inside the metal is now defined as $Y_M(k_z) = -i\epsilon(\omega)k_0/q_V$.

Imposing continuity of the EM fields at the cylindrical wire surface, we obtain the condition for the existence of nonzero solutions for the electric field amplitudes, E_V and E_M . This condition yields the dispersion relation of the SPP modes supported by the structure

$$q_V \frac{K_0(q_V R)}{K_1(q_V R)} = -\frac{q_M}{\epsilon(\omega)} \frac{I_0(q_M R)}{I_1(q_M R)} \quad (3)$$

where R is the radius of the metallic wire.

In Fig. 1, the dispersion relations of the azimuthally-independent SPPs supported by lossless Au wires of different R calculated from Eq. (3) are plotted. The gold dielectric function considered in our calculations is taken from the experimentally fitted Drude–Lorentz-like formula of ref. [28]. We take only the real part of the complex Au ϵ neglecting absorption effects inside the metallic wire. The wires radii (R) range from 0.02 μm (cyan short-dashed line) to 10 μm (green dashed line). It is worth commenting that the SPPs dispersion relation for the $R = 10 \mu\text{m}$ wire coincides with the SPPs supported by a lossless Au flat surface, whereas for narrower wires, the frequency of the SPPs grows more slowly with increasing k_z , leading to stronger localization to the wire.

In the inset of Fig. 1, the radial dependence of $E_r^V = (k_z/k_0)H_\theta^V$ associated to the SPPs supported by metallic wires of radius $R = 0.35 \mu\text{m}$ at 330 THz is depicted. The wine-colored short dashed line shows the field decay for a lossless Au wire ($\epsilon = -34$ for gold at 330 THz). It can be observed how for increasing absolute values of the dielectric constant, $\epsilon = -200$ (grey dotted-dashed line), $\epsilon = -400$ (magenta dotted line), and $\epsilon = -1000$ (dark cyan solid line), while E_r^V tends to the $1/r$

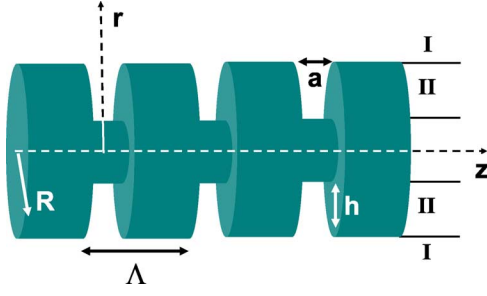


Fig. 2. Schematic picture of the structure supporting cylindrical spoof SPPs: a perfect conducting wire of radius R perforated with a periodic array of rings.

dependence (black dashed line) expected for a perfect conducting wire. This asymptotic behavior can be obtained from (3) taking $\epsilon \rightarrow -\infty$. The dispersion relation of the surface modes supported by the structure approaches the light line ($k_0 \rightarrow k_z$, $q_V \rightarrow 0$). As a result, EM fields are expelled out from the wire, while in the vacuum region, $E_r^V = H_r^V \propto K_1(q_V r) \rightarrow 1/r$ [29]. It can be easily demonstrated that these asymptotic EM fields do not satisfy Gauss law in the absence of free charges. Thus, we can conclude that perfect conducting wires do not support surface EM modes [30].

III. SPOOF SURFACE PLASMONS ON CORRUGATED PERFECT CONDUCTING WIRES

Now that we have seen that uncorrugated metallic wires do not support SPPs in the $\epsilon \rightarrow -\infty$ limit, in this section, we analyze in detail the formation of surface EM modes on periodically corrugated perfect conducting wires [31] (the cylindrical analog of the so-called spoof SPPs on a corrugated perfect conducting 2D plane [22], [23]).

We develop a modal expansion formalism, an extension of the one applied in the aforesaid section, in order to solve Maxwell equations for the structure schematically depicted in Fig. 2: a perfect conducting wire of radius R drilled with a periodic array of subwavelength rings. We introduce the term *metawire* for such a structure, as the emergence of the electromagnetic surface mode can be viewed in a context of metamaterials. We label the array period as Λ , and the rings width and depth as a and h , respectively. Taking advantage of the periodic character of the structure, we can apply Bloch's theorem to the problem and solve Maxwell equations only inside the unit cell of length Λ (see Fig. 2). Within this unit cell, EM fields are nonzero only in the vacuum region surrounding the wire (region I), and inside the perforated rings (region II). As in the previous section, in our analysis, we will look for azimuthally-independent p -polarized surface modes. Under this constraint, EM fields in region I can be expressed as a sum over diffraction modes in the z -direction whose radial dependence is again given by the modified Bessel functions of the second kind

$$\begin{aligned} E_z^I(r, z) &= \sum_{n=-\infty}^{\infty} C_n K_0(q_n^I r) \phi_n(z) \\ H_\theta^I(r, z) &= \sum_{n=-\infty}^{\infty} Y_n^I C_n K_1(q_n^I r) \phi_n(z) \end{aligned} \quad (4)$$

where now, $k_n = k_z + n \frac{2\pi}{\Lambda}$ and $q_n^I = \sqrt{k_n^2 - k_0^2}$. $Y_n^I = ik_0/q_n^I$ is the admittance of the Bloch wave $\phi_n(z) = \frac{e^{ik_n z}}{\sqrt{\Lambda}}$.

Inside the rings, EM fields can be expanded as a sum over propagating and counterpropagating waveguide modes in r -direction as

$$\begin{aligned} E_z^{II}(r, z) &= \sum_l D_l (J_0(q_l^{II} r) - \alpha_l N_0(q_l^{II} r)) \chi_l(z) \\ H_\theta^{II}(r, z) &= \sum_l Y_l^{II} D_l (J_1(q_l^{II} r) - \alpha_l N_1(q_l^{II} r)) \chi_l(z) \end{aligned} \quad (5)$$

where $q_l^{II} = \sqrt{k_0^2 - (l\pi/a)^2}$ and $Y_l^{II} = -ik_0/q_l^{II}$. The ring waveguide modes are given by $\chi_l(z) = \sqrt{(2 - \delta_{l,0})/a} \cos \frac{l\pi}{a} (z + a/2)$ for $|z| < a/2$ (inside the ring) and $\chi_l(z) = 0$, otherwise. The radial dependence of these modes is described by Bessel and Neumann functions $J_{0,1}$ and $N_{0,1}$. The constant $\alpha_l = J_0[q_l^{II}(R-h)]/N_0[q_l^{II}(R-h)]$ is defined so that the electric field satisfies perfect conducting boundary conditions at the ring bottom [$E_z(r=R-h) = 0$].

We impose continuity to the EM fields at the wire outer radius interface ($r = R$). The z -component of the electric field must be continuous everywhere on the interface, whereas the θ -component of the magnetic field is continuous only at the rings openings. Projecting the electric continuity equations over Bloch modes, and the equations linked to the magnetic field continuity over ring waveguide modes, we remove the dependence on z of the matching equations. Defining the quantities

$$E_l = D_l (J_0(q_l^{II} R) - \alpha_l N_0(q_l^{II} R)) \quad (6)$$

which are related to the l -modal amplitude associated with the z -component of the electric field at the rings apertures, the set of EM fields continuity equations can be rewritten as

$$(G_{ll} - \epsilon_l) E_l + \sum_{s \neq l} G_{ls} E_s = 0 \quad (7)$$

where l and s labels the ring waveguide mode order. The different terms appearing in this set of linear equations have a simple physical interpretation. The term

$$\epsilon_l \equiv Y_l^{II} \frac{J_1(q_l^{II} R) - \alpha_l N_1(q_l^{II} R)}{J_0(q_l^{II} R) - \alpha_l N_0(q_l^{II} R)} \quad (8)$$

describes all the bouncing processes experienced by the EM fields linked to mode l along the radial direction inside the rings, whereas

$$G_{ls} \equiv \sum_{n=-\infty}^{\infty} Y_n^I \frac{K_1(q_n^I R)}{K_0(q_n^I R)} \Omega_{ln} \Omega_{sn}^* \quad (9)$$

takes into account the EM radiation emitted by waveguide mode m into vacuum Bloch waves and collected by mode l , with $\Omega_{ln} = \int \chi_l(z) \phi_n(z) dz$ being the overlap integral between the waveguide mode l and the n -Bloch mode. It controls the coupling between EM fields associated to different ring waveguide modes.

Once the set of homogeneous matching equations (7) has been built up, the dispersion relation of the spoof SPPs supported by the ring array is given by the nonzero solutions of the

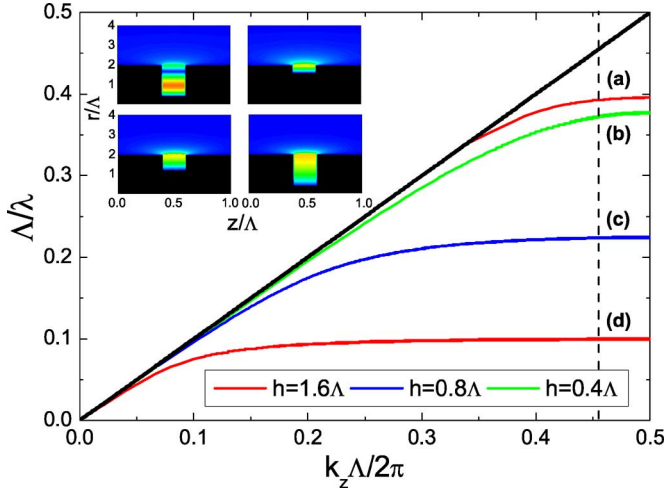


Fig. 3. Normalized ω versus k_z for the θ -independent spoof SPPs supported by perforated wires of radius $R = 2\Lambda$ for three different ring depths. For all the structures, the ring width is $a = 0.2\Lambda$. Inset: Electric field pattern at $k_z = 0.455(2\pi/\Lambda)$ associated to the four SPP bands shown in the main panel.

electric field modal amplitudes E_l . Here, we introduce a further approximation in our theoretical analysis by assuming that the wavelength of the light is much larger than the rings width ($\lambda = 2\pi/k_0 \gg a$). In previous papers [32]–[34], it has been demonstrated that within this subwavelength regime, it is a very good approximation to consider only the first waveguide mode (here, $l = 0$) inside the cavity perforated on the perfect conducting surface (note that in this case, irrespective of the ratio between a and λ , this first waveguide mode is always propagating). Within this approximation, the condition $(G_{00} - \epsilon_0) = 0$ gives the dispersion relation ($\omega(k_z)$) of the azimuthally-independent spoof SPPs propagating along the structure, which can be written as

$$\sum_{n=-\infty}^{\infty} \frac{k_0 K_1(q_n^I R)}{q_n^I K_0(q_n^I R)} |\Omega_{0n}|^2 = -\frac{J_1(k_0 R) - \alpha_0 N_1(k_0 R)}{J_0(k_0 R) - \alpha_0 N_0(k_0 R)} \quad (10)$$

where $\Omega_{0n} = \sqrt{\frac{a}{\Lambda}} \text{sinc}(k_n a/2)$ is the overlap integral between the first ring waveguide mode and the n -Bloch wave.

In Fig. 3, the spoof SPP bands for three different ring arrays are plotted. Since we are considering perfect conducting boundary conditions, all lengths within the structures are scalable and we can take the period Λ as the unit length. The perforated wire radius is $R = 2\Lambda$, and the ring width $a = 0.2\Lambda$. The three ring depths considered in the calculations are: $h = 1.6\Lambda$ (red solid line), $h = 0.8\Lambda$ (green dotted line), and $h = 0.4\Lambda$ (blue dashed line). We can observe how the spoof SPP dispersion relation departs from the light line, resembling the behavior of SPPs propagating along metallic wires at optical frequencies (see Fig. 1).

At low frequencies ($\lambda \gg \Lambda, a$), and for wires much thicker and rings much shallower than the array period ($R, R - h \gg \Lambda$), we can obtain an analytical expression for the spoof SPP dispersion relation by introducing the asymptotic expansions of

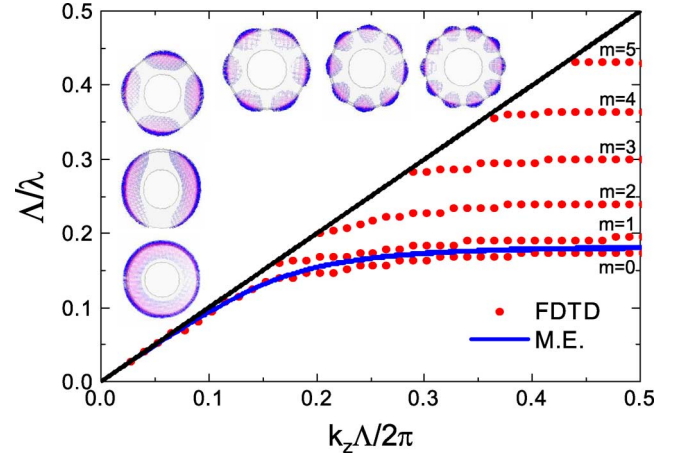


Fig. 4. Spoof SPP dispersion relation including all the different azimuthal behaviors (labeled with m) supported by a perfect conducting wire of radius $R = 2\Lambda$ drilled with rings of width $a = 0.2\Lambda$ and depth $h = 0.5\Lambda$. The insets show the electric field amplitude at $k = \pi/\Lambda$ associated to the different bands with m running from the left bottom corner to the right top corner of the figure.

the different Bessel functions involved in (10), obtaining

$$k_z = k_0 \sqrt{1 + \left(\frac{a}{\Lambda}\right)^2 \tan^2(k_0 h)}. \quad (11)$$

This expression coincides with that given in [23] for spoof SPPs propagating along a perfect conductor surface perforated with an 1-D array of grooves of width a and depth h . As seen in Fig. 3, the key parameter governing the surface EM mode confinement is the depth of the rings, h .

It is well known that the dispersion relation of SPPs in a flat 2-D surface approaches $\omega_s = \omega_p/\sqrt{2}$ (where ω_p is the plasma frequency of the metal) as the parallel momentum is increased. In the case of a periodically perforated perfect conductor wire, it is possible to define an analogous asymptotic frequency, ω_s . An analytical expression for ω_s can be extracted from (11) by imposing the condition $\tan(k_0 h) \rightarrow \infty$, obtaining $\omega_s = \pi c/2h$. This inversely proportional dependence of ω_s with h gives rise to a lowering of the spoof SPP bands as h is increased. This fact can be observed in bands (b)–(d) of Fig. 3. The electric field associated to these modes do not present any node in r -direction (see the inset of Fig. 3) and the flat region of $\omega(k_z)$ occurs at lower frequencies as the rings depth is enlarged. For $h = 1.6\Lambda$, another band linked to a spoof SPP mode presenting a radial node inside the ring [see inset (a)] appears at larger frequencies. Although the condition $R - h \gg \Lambda$ is not fulfilled, we can associate it to another asymptotic frequency $\omega_s = 3(\pi c/2h)$ also satisfying $\tan(k_0 h) \rightarrow \infty$.

In Fig. 4, the dispersion relation of the spoof SPPs supported by a perfectly conducting wire of radius $R = 2\Lambda$ perforated by a periodic array of rings of dimensions $a = 0.2\Lambda$ and $h = \Lambda$ is depicted. In this calculation, there is no restriction regarding the azimuthal dependence of the EM fields. The dispersion relation (red dots) has been obtained by means of a 3-D FDTD numerical calculation. The number of mesh points considered in the calculation are $240 \times 240 \times 40$, with a mesh size equal to 0.08Λ . The different bands (labeled with index m) correspond

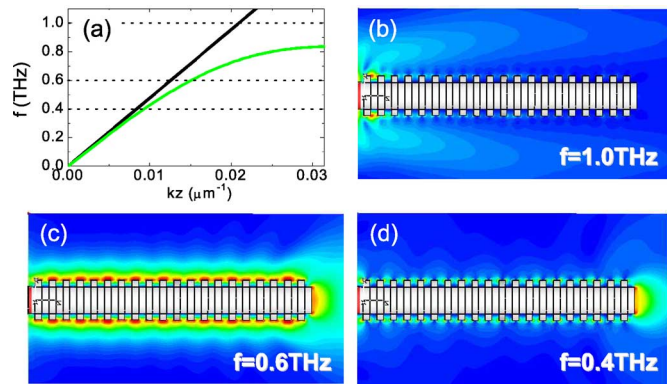


Fig. 5. Quasi-analytical dispersion relation (a) and electric field plots (b–d) for terahertz spoof SPPs propagating along a metawire of radius $R = 150 \mu\text{m}$ perforated by an array of ring of period $\Lambda = 100 \mu\text{m}$. The ring's width and depth are $50 \mu\text{m}$. Dotted lines show the three different frequencies (1.0, 0.6, and 0.4 THz) considered in the (FIT) simulations of the averaged electric field amplitude for metawires of length $20 \times \Lambda$ illuminated from the left by a radially polarized plane wave.

to different azimuthal symmetries of the electric field amplitude shown in the insets of the figure. For the structure considered, m ranges from $m = 0$ (θ -independent SPPs) to $m = 5$ (insets from left bottom corner to right top corner of Fig. 4). The electric field associated to the m^{th} azimuthal mode presents $2m$ nodes and/or maxima in θ . The solid blue line shows the $m = 0$ band calculated from (10). We can see the very good agreement between the numerical and quasi-analytical results for the azimuthally-independent spoof SPP dispersion relation.

IV. GUIDING AND FOCUSING OF LIGHT BY MEANS OF CYLINDRICAL SPOOF SURFACE PLASMONS

One of the possible applications of these cylindrical spoof SPPs is to guide EM radiation with frequencies lying within the microwave or THz ranges of the EM spectrum along a metallic wire. This functionality is illustrated in Fig. 5.

In this case, the geometry of the ring array (period, width, and depth of the rings) is chosen such that the optimal frequencies for guiding would be around 0.6–0.8 THz. Panel (a) shows the dispersion relation of the spoof SPPs supported by the infinite structure, whereas panels (b)–(d) depict the E-field amplitude patterns (evaluated at three different frequencies) for a finite version of the structure (containing 20 periods) illuminated by a radially polarized broadband terahertz pulse. These pictures have been obtained by numerical simulations using a finite integration technique (FIT). As clearly seen in this figure, for the lowest frequency considered, $f = 0.4$ THz, as k_z is close to the light line, the guiding properties are poor in comparison with the frequency $f = 0.6$ THz in which the EM radiation is guided and strongly confined along the wire surface. At $f = 1.0$ THz, no spoof SPPs are supported by the system [see Fig. 5(a)] and the incident radiation is scattered at the left entrance.

By taking advantage of the dependence of the spoof SPP confinement on the geometry of the ring array, it is feasible to design a periodically corrugated wire that is able to concentrate EM energy at the end of the cylindrical wire. In this paper, we

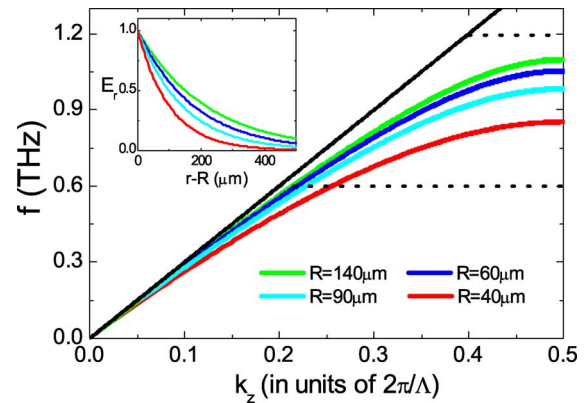


Fig. 6. Frequency versus parallel wavevector for spoof SPPs supported by metawires of different radii perforated with periodic ring arrays of period $\Lambda = 100 \mu\text{m}$ and ring dimensions $a = 50 \mu\text{m}$ and $h = 30 \mu\text{m}$. Dotted lines indicate two different frequencies (0.6 and 1.2 THz). Inset: Electric field radial component versus $r - R$ at $f = 0.6$ THz for the four infinite metawires considered in the main panel.

present just one possible structure. It is a conical wire, in which the external radius is gradually decreased along the wire but the depth of the rings is fixed.

In Fig. 6, we render the dispersion relation of the spoof SPPs supported by infinite cylindrical wires in which the depth of the rings ($h = 30 \mu\text{m}$), their width $a = 50 \mu\text{m}$, and the period of the array $\Lambda = 100 \mu\text{m}$ are fixed. The four curves correspond to dispersion relation for four different values of R , ranging from $R = 140 \mu\text{m}$ to $R = 40 \mu\text{m}$. As expected, as R is decreased, the dispersion relation departs more and more from the light line. This implies that the confinement of the corresponding surface EM mode is increased as R is reduced, as can be seen in the inset of the figure, which shows the radial component of the E-field (E_r) as a function of the distance to the wire ($r - R$). This magnitude is evaluated at $f = 0.6$ THz for the four different structures.

Therefore, it is expected that if we construct a finite metawire in which the depth of the grooves is fixed and the external radius is gradually reduced from $R = 140 \mu\text{m}$ to $R = 40 \mu\text{m}$, EM radiation of frequency $f = 0.6$ THz will be focused at the end of the conical wire. This focusing effect is nicely demonstrated in Fig. 7, which shows FIT simulations on a conical wire of length 2 mm (that contains 20 periods of the ring array) for two different frequencies $f = 0.6$ THz and $f = 1.2$ THz. As expected from the calculations for infinite wires, at $f = 0.6$ THz EM radiation is guided along the wire and focused as it propagates through it. As a comparison, we also depict the E-field pattern for $f = 1.2$ THz in which EM is scattered at the entrance of the wire due to the nonexistence of spoof SPPs at that particular frequency. It is worth noticing that focusing is also expected to occur with smooth tapered wires [35]. However, in this case, significant losses into the radiation continuum can be expected for fabricated structures due to scattering of the weakly confined modes at surface imperfections. Even for the case of a perfectly smooth interface, a detailed comparison of the mode focusing characteristics between smooth and metawire tapers in terms of efficiency has yet to be performed.

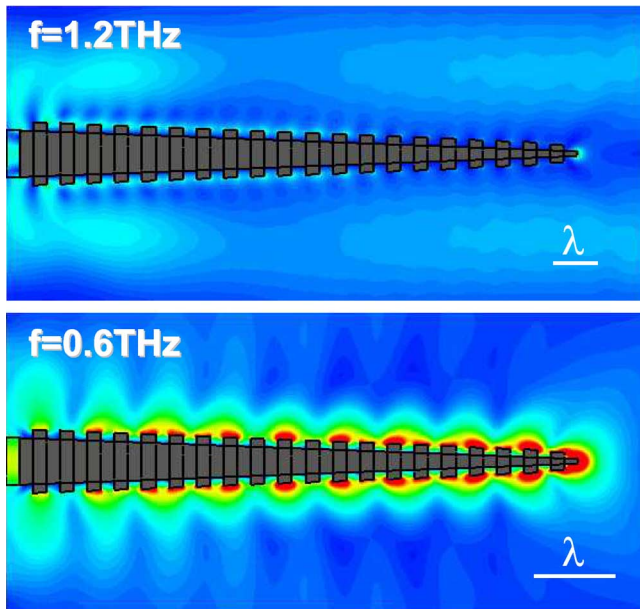


Fig. 7. Focusing and guiding of light through spoof SPPs propagating along a perfect conducting cone of length 2 mm corrugated by a ring array in which the radius is gradually reduced from $R = 140 \mu\text{m}$ to $R = 40 \mu\text{m}$. As expected from the dispersion relation of Fig. 6, spoof SPPs are excited at $f = 0.6 \text{ THz}$, while at $f = 1.2 \text{ THz}$ these surface EM modes are not supported by the structure.

V. CONCLUSION

In conclusion, we have presented a detailed study of the surface electromagnetic modes that can propagate along a periodically corrugated perfect conductor wire. Firstly, we have analyzed the SPPs supported by an uncorrugated metallic wire at optical frequencies. Although the confinement of these modes disappears as we approach to the limit $\epsilon \rightarrow -\infty$, the confinement is recovered when the surface of the perfect conductor is corrugated with a periodic array of rings. We have shown how the dispersion characteristics of these geometry-induced surface electromagnetic modes is completely governed by the depth of the rings. This allows guiding radiation at microwave or THz frequencies along a corrugated wire. Moreover, by a clever design of the corrugation along the wire, it is possible to focus electromagnetic energy of a given frequency at the end of the wire. We strongly believe that these ideas will find important applications in the THz or microwave ranges of the electromagnetic spectrum, enabling a new class of research and technology in which the tunability of the guiding properties of the spoof SPPs will play a key role.

REFERENCES

- [1] S. A. Maier, *Plasmonics—Fundamentals and Applications*, 1st ed. New York: Springer, 2007.
- [2] S. Lal, S. Link, and N. J. Halas, “Nano-optics from sensing to waveguiding,” *Nat. Photon.*, vol. 1, pp. 641–648, Nov. 2007.
- [3] A. Sommerfeld, “Ueber die Fortpflanzung elektrodynamischer Wellen laengs eines Drahtes,” *Ann. Phys. Chem.*, vol. 67, pp. 233–290, 1899.
- [4] U. Fano, “The theory of anomalous diffraction gratings and of quasi-stationary waves on metallic surfaces (Sommerfeld’s waves),” *J. Opt. Soc. Am.*, vol. 31, pp. 213–222, Mar. 1941.
- [5] R. H. Ritchie, “Plasma losses by fast electrons in thin films,” *Phys. Rev.*, vol. 106, no. 5, pp. 874–881, Jun. 1957.
- [6] S. A. Maier, M. L. Brongersma, P. G. Kik, S. Meltzer, A. A. G. Requicha, and H. A. Atwater, “Plasmonics—A route to nanoscale optical devices,” *Adv. Mater.*, vol. 13, no. 19, pp. 1501–1506, Oct. 2001.
- [7] J. Takahara, S. Yamagishi, H. Taki, A. Morimoto, and T. Kobayashi, “Guiding of a one-dimensional optical beam with nanometer diameter,” *Opt. Lett.*, vol. 22, no. 7, pp. 475–477, Apr. 1997.
- [8] R. M. Dickson and L. A. Lyon, “Unidirectional plasmon propagation in metallic nanowires,” *J. Phys. Chem. B*, vol. 104, pp. 6095–6098, 2000.
- [9] J. R. Krenn, B. Lamprecht, H. Ditlbacher, G. Schider, M. Salerno, A. Leitner, and F. R. Aussenegg, “Non-diffraction-limited light transport by gold nanowires,” *Europhys. Lett.*, vol. 60, no. 5, pp. 663–669, Dec. 2002.
- [10] S. A. Maier, P. G. Kik, H. A. Atwater, S. Meltzer, E. Harel, B. E. Koel, and A. A. G. Requicha, “Local detection of electromagnetic energy transport below the diffraction limit in metal nanoparticle plasmon waveguides,” *Nat. Mater.*, vol. 2, no. 4, pp. 229–232, Apr. 2003.
- [11] F. López-Tejeda, S. G. Rodrigo, L. Martín-Moreno, F. J. García-Vidal, E. Devaux, T. W. Ebbesen, J. R. Krenn, I. P. Radko, S. I. Bozhevolnyi, M. U. González, J. C. Weeber, and A. Dereux, “Efficient unidirectional nanoslit couplers for surface plasmons,” *Nat. Phys.*, vol. 3, pp. 324–328, 2007.
- [12] S. I. Bozhevolnyi, V. S. Volkov, E. Devaux, J.-Y. Laluet, and T. W. Ebbesen, “Channel plasmon subwavelength waveguide components including interferometers and ring resonators,” *Nature*, vol. 440, pp. 508–511, 2006.
- [13] S. M. Nie and S. R. Emery, “Probing single molecules and single nanoparticles by surface-enhanced Raman scattering,” *Science*, vol. 275, no. 5303, pp. 1102–1106, 1997.
- [14] K. Kneipp, Y. Wang, H. Kneipp, L. T. Perelman, I. Itzkan, R. R. Dasari, and M. S. Feld, “Single molecule detection using surface-enhanced Raman scattering (SERS),” *Phys. Rev. Lett.*, vol. 78, no. 9, pp. 1667–1670, 1997.
- [15] J. Zenneck, “Ueber die Fortpflanzung ebener elektromagnetischer Wellen laengs einer ebenen Leiterflaeche und ihre Beziehung zur drahtlosen Telegraphie,” *Annu. Phys.*, vol. 23, pp. 846–866, 1907.
- [16] K. Wang and D. M. Mittleman, “Metal wires for terahertz wave guiding,” *Nature*, vol. 432, pp. 376–379, Nov. 2005.
- [17] T.-I. Jeon, J. Zhang, and D. Grischkowsky, “THz Sommerfeld wave propagation on a single metal wire,” *Appl. Phys. Lett.*, vol. 86, p. 161904, 2005.
- [18] G. Goubau, “Surface waves and their application to transmission lines,” *J. Appl. Phys.*, vol. 21, pp. 1119–1128, Nov. 1950.
- [19] G. Piefke, “The transmission characteristics of a corrugated guide,” *IRE Trans. Antennas Propag.*, vol. 7, no. 5, pp. 183–190, 1959.
- [20] D. L. Mills and A. A. Maradudin, “Surface corrugation and surface-polariton binding in the infrared frequency range,” *Phys. Rev. B, Condens. Matter*, vol. 39, pp. 1569–1574, Jan. 1989.
- [21] R. Ulrich and M. Tacke, “Submillimeter waveguiding on periodic metal structure,” *Appl. Phys. Lett.*, vol. 22, pp. 251–253, Mar. 1973.
- [22] J. B. Pendry, L. Martín-Moreno, and F. J. García-Vidal, “Mimicking surface plasmons with structured surfaces,” *Science*, vol. 305, pp. 847–848, Aug. 2004.
- [23] F. J. García-Vidal, L. Martín-Moreno, and J. B. Pendry, “Surfaces with holes in them: New plasmonic metamaterials,” *J. Opt. A: Pure Appl. Opt.*, vol. 7, pp. S97–S101, 2005.
- [24] F. J. García de Abajo and J. J. Saenz, “Electromagnetic surface modes in structured-conductor surfaces,” *Phys. Rev. Lett.*, vol. 95, no. 23, p. 233901, Dec. 2005.
- [25] S. A. Maier and S. R. Andrews, “Terahertz pulse propagation using plasmon-polariton-like surface waves on structured conductive surfaces,” *Appl. Phys. Lett.*, vol. 88, no. 20, p. 251120, Jun. 2006.
- [26] C. A. Pfeiffer, E. N. Economou, and K. L. Ngai, “Surface polaritons in a circularly cylindrical interface: Surface plasmons,” *Phys. Rev. B*, vol. 10, no. 8, pp. 3038–3049, 1974.
- [27] L. Novotny and C. Hafner, “Light propagation in a cylindrical waveguide with complex, metallic, dielectric function,” *Phys. Rev. B, Condens. Matter*, vol. 50, no. 5, pp. 4094–4106, 1994.
- [28] A. Vial, A.-S. Grimault, D. Macias, D. Barchiesi, and M. L. de la Chapelle, “Improved analytical fit of gold dispersion: Application to the modelling of extinction spectra with a finite-difference time-domain method,” *Phys. Rev. B, Condens. Matter*, vol. 71, p. 085416, 2005.
- [29] G. B. Arfken and H. J. Weber, *Mathematical Methods for Physicists*, 5th ed. London, U.K.: Harcourt Academic, 2001.
- [30] J. D. Jackson, *Classical Electrodynamics*, 3rd ed. New York: Wiley, 1999, p. 358.

- [31] S. A. Maier, S. R. Andrews, L. Martín-Moreno, and F. J. García-Vidal, "Terahertz surface plasmon-polariton propagation and focusing on periodically corrugated wires," *Phys. Rev. Lett.*, vol. 97, p. 056402, 2006.
- [32] C. C. Chen, "Transmission through a conducting screen perforated periodically with apertures," *IEEE Trans. Microw. Theory Tech.*, vol. MTT-18, no. 9, pp. 627–632, Sep. 1970.
- [33] R. C. McPhedran and D. Maystre, "On the theory and solar application of inductive grids," *Appl. Phys. B, Photophys. Laser Chem.*, vol. 14, no. 1, pp. 1–20, Sep. 1977.
- [34] J. A. Porto, F. J. Garcia-Vidal, and J. B. Pendry, "Transmission resonances on metallic gratings with very narrow slits," *Phys. Rev. Lett.*, vol. 83, no. 14, pp. 2845–2848, Oct. 1999.
- [35] J. A. Deibel, M. Escarra, N. Berndsen, K. Wang, and D. M. Mittleman, "Finite-element method simulations of guided wave phenomena at terahertz frequencies," *Proc. IEEE*, vol. 95, no. 8, pp. 1624–1640, Aug. 2007.



A. I. Fernández-Domínguez received the M.S. degree in physics from the Universidad Autónoma de Madrid, Madrid, Spain, in 2004, where he is currently working toward the Ph.D. degree in the Departamento de Física Teórica de la Materia Condensada.



L. Martín-Moreno received the M.S. and Ph.D. degrees in physics from the Universidad Autónoma de Madrid, Madrid, Spain, in 1985 and 1989, respectively.

Since 1994, he has been an Associate Professor in the Departamento de Física de la Materia Condensada, Universidad de Zaragoza, Zaragoza, Spain.



F. J. García-Vidal received the Ph.D. degree from the Universidad Autónoma de Madrid, Madrid, Spain, in 1992.

Since 1994, he has been working in the field of plasmonics. He is currently a Full Professor in the Departamento de Física Teórica de la Materia Condensada, Universidad Autónoma de Madrid.



S. R. Andrews received the B.A. and D.Phil. degrees from Oxford University in 1979 and 1982 respectively.

He joined the University of Edinburgh as a Research Fellow in 1982, where he was engaged in research on phase transitions. He then moved to the Long-Range Research Division of GEC-Marconi in 1985, where he was engaged in research on the physics and device applications of low-dimensional semiconductors. After two years as a Royal Society Industrial Fellow in Cambridge, he joined the University of Bath in 1994.

His current research interests include the fields of terahertz photonics and ultrafast studies of semiconductors and metamaterials.



S. A. Maier received the Ph.D. degree in applied physics from the California Institute of Technology, Pasadena, in 2003.

He is currently a Reader in the Experimental Solid State Group, Department of Physics, Imperial College, London U.K.